PHILOSOPHICAL TRANSACTIONS A

Review

Check for updates

Author for correspondence:
Sandy J. Thomalla
e-mail: sandy.thomalla@gmail.com

Southern Ocean phytoplankton dynamics and carbon export: insights from a seasonal cycle approach

Sandy J. Thomalla[1,2], Marcel Du Plessis[4], Nicolas Fauchereau[5], Isabelle Giddy[1,3], Luke Gregor[6], Stephanie Henson[7], Warren R. Joubert[8], Hazel Little[3], Pedro M. S. Monteiro[1,10], Thato Mtshali[9], Sarah Nicholson[1], Thomas J. Ryan-Keogh[1] and Sebastiaan Swart[4,3]

[1]Southern Ocean Carbon-Climate Observatory, CSIR, Cape Town, South Africa
[2]Marine and Antarctic Research Centre for Innovation and Sustainability, and [3]Department of Oceanography, University of Cape Town, Cape Town, South Africa
[4]Department of Marine Sciences, University of Gothenburg, Göteburg, Sweden
[5]The National Institute of Water and Atmospheric Research, Hamilton, New Zealand
[6]Environmental Physics Group, ETH Zürich, Institute of Biogeochemistry and Pollutant Dynamics, Zurich, Switzerland
[7]National Oceanography Centre, Southampton, UK
[8]South African Weather Service, Cape Town, South Africa
[9]Department of Forestry, Fisheries and the Environment, Oceans and Coast, Cape Town, South Africa
[10]School for Climate Studies, Stellenbosch University, Stellenbosch, South Africa

iD SJT, 0000-0002-6802-520X; MDP, 0000-0003-2759-2467; SS, 0000-0002-2251-8826

Quantifying the strength and efficiency of the Southern Ocean biological carbon pump (BCP) and its response to predicted changes in the Earth's climate is fundamental to our ability to predict long-term changes in the global carbon cycle and,

THE ROYAL SOCIETY
PUBLISHING

by extension, the impact of continued anthropogenic perturbation of atmospheric CO_2. There is little agreement, however, in climate model projections of the sensitivity of the Southern Ocean BCP to climate change, with a lack of consensus in even the direction of predicted change, highlighting a gap in our understanding of a major planetary carbon flux. In this review, we summarize relevant research that highlights the important role of fine-scale dynamics (both temporal and spatial) that link physical forcing mechanisms to biogeochemical responses that impact the characteristics of the seasonal cycle of phytoplankton and by extension the BCP. This approach highlights the potential for integrating autonomous and remote sensing observations of fine scale dynamics to derive regionally optimized biogeochemical parameterizations for Southern Ocean models. Ongoing development in both the observational and modelling fields will generate new insights into Southern Ocean ecosystem function for improved predictions of the sensitivity of the Southern Ocean BCP to climate change.

This article is part of a discussion meeting issue 'Heat and carbon uptake in the Southern Ocean: the state of the art and future priorities'.

1. Background and rationale

The inertia of a flywheel opposes and moderates fluctuations and stores excess energy. As such, the Southern Ocean can be considered the climate flywheel of the planet, buffering the impacts of climate change by accounting for 50% of the total oceanic uptake of anthropogenic CO_2 [1,2] and 75% of the excess heat generated by anthropogenic CO_2 [3]. The air-sea exchange of CO_2 in the Southern Ocean is balanced by an interplay of physical and biological processes that vary on a seasonal cycle. Typically, the Southern Ocean is characterized by a dominance of CO_2 outgassing in winter driven by upwelling and mixed layer entrainment of carbon-rich deep water (e.g. [4,5]), whereas in summer, when phytoplankton primary production and carbon export to the deep ocean are at their peak, the biological carbon pump (BCP) dominates CO_2 uptake [6]. Indeed, the Southern Ocean BCP, which includes the physical processes that transport organic material from surface waters to depth, i.e. sinking and subduction, is considered a major contributor to the sink of natural CO_2 removing an estimated 3 Pg of carbon from surface waters south of 30° S each year (i.e. 33% of the global organic carbon flux) [7]. Annually averaged, the global BCP offsets the flux of upwelled pre-industrial dissolved inorganic carbon (DIC) [8,9]. If the contribution that the Southern Ocean BCP makes to offsetting the upwelling of DIC is modified by climate change, it would conceivably begin to play an important role in the net uptake of anthropogenic CO_2 and hence directly impact global climate [10–13]. In addition, although the magnitude of the feedback is under debate (e.g. [6]), it is widely agreed that the Southern Ocean BCP plays an important role in regulating the supply of nutrients to thermocline waters (Subantarctic Mode Water and Intermediate Water) of the Southern Hemisphere and North Atlantic [14,15], which in turn drives low latitude productivity and associated carbon export [16]. As such, any reduction in the efficiency of the Southern Ocean BCP has the potential to be one of the most important positive feedbacks on global climate change [17].

It is anticipated that anthropogenic forcing will increasingly influence oceanic nutrient cycling [18] impacting primary production, ecosystem function and the transfer of carbon, energy and nutrients through pelagic and benthic food webs with complex feedbacks on ocean biogeochemistry and climate [19,20]. The Southern Ocean is considered to be particularly sensitive to climate change [21] with widespread physico-chemical changes already being observed in regional warming [22], freshening linked to changes in sea ice extent [23], increased vertical stratification and altered mixed layer depths (MLDs) in response to stronger winds [24] associated with a more positive phase of the Southern Annular Mode [25]. Understanding how the strength and efficiency of the BCP is expected to respond to these predicted changes is

necessary for accurately predicting long-term trends in the global carbon cycle and by extension global climate [13,26–28]. Nevertheless, the processes and dynamics that define the direction, the magnitude and the rates of change of the Southern Ocean BCP (i.e. the climate sensitivity) are not well understood [12,27,28]. There is little consensus in even the direction of predicted change in the Southern Ocean BCP (from coupled model intercomparison project phase 6 predictions), highlighting gaps in our knowledge of a major planetary carbon flux [27].

The seasonal cycle provides a contemporary observable lens to investigate the links between seasonal changes in buoyancy and momentum forcing of mixed layer physics and ecosystem response in terms of production and associated carbon export [29–33]. Accordingly, it is thought that the variability and long-term trends in mean annual Southern Ocean productivity may be mediated through changes in the characteristics of its seasonal cycle [29,34]. The coupling of these physical and biogeochemical processes at seasonal scales may also be used as part of emergent constraints analyses to reduce uncertainty in long-term projections of ocean productivity and CO_2 flux [35].

Two decades ago, a review by Boyd [36] used key observational and experimental data sources to provide a seasonal framework for understanding the complex temporal and spatial patterns of environmental factors that control the distribution of phytoplankton stocks, species composition and their physiological status in the Southern Ocean. A key outcome (based on the work of Boyd *et al.* [37]; Franck *et al.* [38]; Nelson *et al.* [39]; Tortell *et al.* [40] and others) was a schematic that summarized the seasonal progression of environmental controls of phytoplankton that included irradiance, iron, silicic acid and others (yet to be confirmed), recognizing that this framework would vary regionally and depend on the dominant taxa (electronic supplementary material, figure S1).

It was also at this time (1990s to early 2000s) that the role of finer scale processes was becoming apparent in dictating phytoplankton standing stocks through vertical nutrient injection, with a comprehensive review provided by Klein & Lapeyre [41]. In essence, nutrient requirements (from new production estimates) surpassed wintertime convective supply from entertainment [42,43]. Mesoscale eddies were proposed (by Jenkins [44] and later by McGillicuddy *et al.* [42,43]) as the mechanism to resolve the nutrient budget, driving injection that accounts for as much as 20–30% of annual requirements. However, a shortfall still remained. Submesoscale physics, i.e. enhanced vertical velocity associated with strong density and vorticity gradients (at spatial scales of 1–10 km) between and around mesoscale eddies (i.e. fronts, meanders and filaments [45]) were proposed as the additional mechanism needed to close the nutrient budget by driving significant injection from the ocean's interior to the mixed layer [46–48]. Meso and submesoscale processes were also shown to be important for increasing light exposure through enhanced stratification initiating patchy blooms earlier in the season [49].

Fine scales of variability are defined here as processes occurring at spatial scales from the submesoscale (0.1–10 km) to the mesoscale (10–200 km) and at temporal scales of days to months (intra-seasonal to seasonal) [50]. These fine scales of variability were highlighted in an observational study by Thomalla *et al.* [29] that used the characteristics of the seasonal cycle of chlorophyll-a (bloom initiation, amplitude and variability) to regionally classify the Southern Ocean. This approach provided a dynamic understanding of the spatial heterogeneity of phytoplankton that emphasized the spatial-temporal prevalence of fine-scale (subseasonal) variability in dictating the characteristics of the seasonal cycle. In particular, the degree of seasonal cycle reproducibility (SCR) (as the % variance explained by the climatological seasonal cycle) provided a useful metric with the ability to capture sub-seasonal scales of variability (figure 1*a*). In regions with high SCR (e.g. in the subtropics), the chlorophyll-a time series was hypothesized to be phase locked to the climatological drivers of seasonal adjustments in light, buoyancy flux and MLD, whereas regions with low SCR (e.g. frontal and marginal ice zones) were proposed as being strongly impacted by intra-seasonal forcing of light and nutrients through smaller scale (spatial and temporal) adjustments in the MLD associated with storms and meso- and submesoscale eddies. A key outcome of this work was a synthesis schematic (figure 1*c*) that divided the Southern Ocean into a mosaic of four regions that summarized the varying response
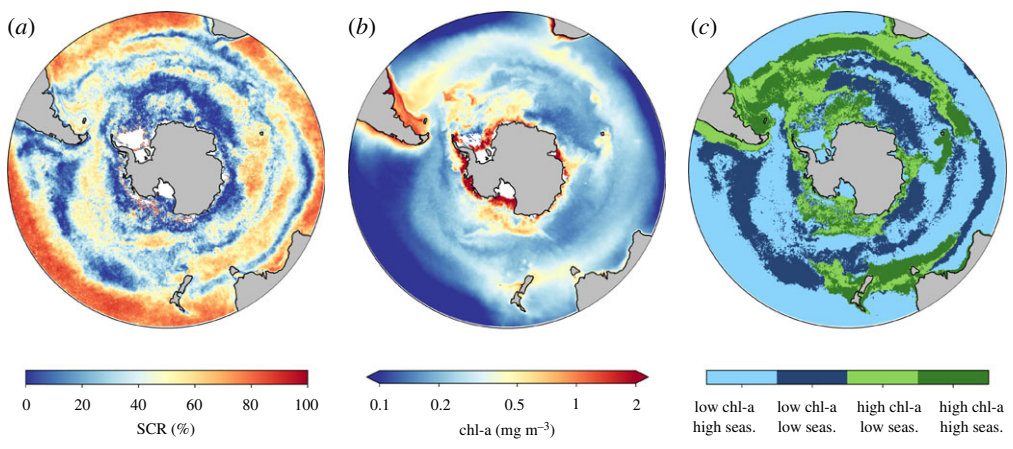
Figure 1. Maps of mean (1999–2009) (*a*) seasonal cycle reproducibility (SCR; %) calculated as defined in Thomalla *et al*. [29], (*b*) chlorophyll-a (mg m^{-3}) and (*c*) a schematic summarizing the response of phytoplankton biomass to the underlying physics of the different seasonal regimes for 1999–2009 as per Thomalla *et al*. [29]. Regions in blue represent regions of low (less than 0.25 mg m^{-3}) chlorophyll-a concentration with either high seasonal cycle reproducibility (greater than 40%) (light blue) or low seasonal cycle reproducibility (less than 40%) (dark blue). Regions in green represent regions of high chlorophyll-a concentration (greater than 0.25 mg m^{-3}) with either low seasonal cycle reproducibility (light green) or high seasonal cycle reproducibility (dark green). Ocean colour data taken from the ocean colour climate change initiative [51].

of phytoplankton biomass (high versus low) to different seasonal regimes (high SCR versus low SCR). Of note were regions of high seasonally integrated biomass (figure 1*b*) coincident with low SCR (figure 1*a*) depicted in light green in figure 1*c*), that were hypothesized to be a consequence of high intra-seasonal physical forcing of the mixed layer (from high wind stress and upper water column stabilization through positive buoyancy forcing associated with mesoscale dynamics) at appropriate time scales to support enhanced phytoplankton growth [29].

The importance of intraseasonal variability in characterizing the seasonal bloom, in particular in the context of wind interactions with meso- and submesoscale physics, was highlighted by a number of other studies during this period. These include high resolution satellite imagery [47] and model simulations [48], which show that an incorrect representation of submesoscale frontogenesis could result in errors in primary production estimates of up to 50% by ignoring transient nutrient inputs from intense submesoscale turbulence forced by high frequency winds [48]. A synthesis of satellite chlorophyll-a, ocean reanalyses and modelling [52] explored the spatial variability in the nature of the chlorophyll-a response to mixing events based on the degree of iron limitation (relative to light) and concluded that the balance between the degree of light and iron limitation dictated the phytoplankton response to transient mixing. Net community production (NCP) measurements (from ΔO_2/Argon ratios) and MLD in the Atlantic Subantarctic Zone (SAZ) [53] implied that NCP variability was driven by alternating states of synoptic scale deepening of the mixed layer that entrained dissolved iron, followed by restratification, allowing rapid growth and high NCP in an iron replete, high light environment. These findings were corroborated by a high-resolution satellite study by Carranza & Gille [54], which confirmed that high winds correlate with high chlorophyll-a over much of the Southern Ocean similarly suggesting that transient MLD deepening (i.e. wind-driven entrainment) helps sustain high chlorophyll-a through much of the Southern Ocean in summer.

Together, these studies (and others around the time) stress the importance of coupling ocean physics to biogeochemistry at high-resolution scales in both time (seasonal to intraseasonal) and space (meso- to submesoscale) in order to resolve the environmental drivers that determine the characteristics of the seasonal cycle. This nuanced understanding expands on the original seasonal framework of Boyd [36] and highlights the necessity for innovative fine-scale

observations (e.g. ocean robotics and satellite remote sensing) that can sample at a frequency appropriate to capture the dominant scales of variability in the physics and the growth timescales of phytoplankton. These observations can be combined with modelling techniques (mechanistic and empirical) to fill gaps in our knowledge at temporal and spatial scales hitherto undersampled and poorly understood in the Southern Ocean.

2. Accessing the fine-scale through autonomous platforms, remote sensing and modelling

(a) Insights from the Southern Ocean carbon and climate observatory

The requirement for fine-scale observations has stimulated the development of integrated modelling and observational approaches, e.g. the Southern Ocean Seasonal Cycle EXperiments: SOSCEx led by the South African Southern Ocean carbon-climate observatory (SOCCO). These experiments merge innovative *in situ* robotics and remote sensing observational capabilities with advanced ship-based experimental infrastructure and high-resolution modelling to observe seasonality through a high-resolution lens. We provide here a synthesis of understanding gained from SOCCO glider deployments in the Atlantic SAZ ([30], figure 2*a–f*), a region of high chlorophyll-a and low SCR (light green region in figure 1*c*), as a case study on how high-resolution observations generated by autonomous underwater vehicles (3 h, 2 km resolution) can be used to address fine-scale physical-biogeochemical interactions.

Although glider observations opened new avenues to sample time and space scales to illuminate our view of the characteristics of the seasonal cycle, a better understanding of their limitations was also required, specifically about how best to interpret the nature of the quasi-Lagrangian time series that is capturing both temporal and spatial scales of variability intrinsic to our interpretation of growth and spatial distribution. A spatio-temporal investigation [55] revealed that chlorophyll-a variability captured by a glider was generally larger than the spatial variability observed in co-located remote sensing images. As such, the variability observed by gliders was considered to be mostly due to sub-daily phytoplankton adjustments in time rather than glider trajectories sampling fine-scale features in space [55].

Contrasting physical-biogeochemical interactions led to a separation of the time series into spring and summer [30] identified as the date when mean stratification above the winter mixed layer persistently increased due to positive net heat flux, while in spring, stratification was comparatively weak and MLDs typically deep (greater than 200 m). That said, meso- to submesoscale eddies and fronts in spring coincided with intermittent (1–2 days) increases in vertical stratification and a rapid shoaling of the mixed layer (greater than 160 m day^{-1}). These restratification events occurred 1–2 months prior to the heat flux becoming net positive and strongly affected the spatially and temporally heterogeneous blooms observed in spring, where the dominant signals of variability were less than 10 days [55]. Here, enhanced light availability through reduced mixing [56–58] contributes to intermittent increased rates of NCP [31]. The role of eddies in driving the rapid variability of mixed layer stratification was confirmed in a study by du Plessis *et al.* [59], who compared the mean stratification of the mixed layer from the glider time series to a one-dimensional numerical simulation forced with wind stress and heat flux for the respective time and position of the glider. Their comparison showed large excursions between observed and modelled stratification during periods where enhanced horizontal buoyancy gradients were observed in the glider time series, which suggests the presence of three-dimensional mechanisms not resolved in the model that plays an important role in explaining enhanced springtime stratification. In a follow up study using four consecutive years of spring-to-summer glider deployments, [60] showed that during periods of strong down-front winds (aligned in the direction of a front), enhanced mixing [61] delayed the onset date of seasonal mixed layer restratification by multiple weeks after the heat flux turned net positive. This restratification date has important implications for the mean light exposure to
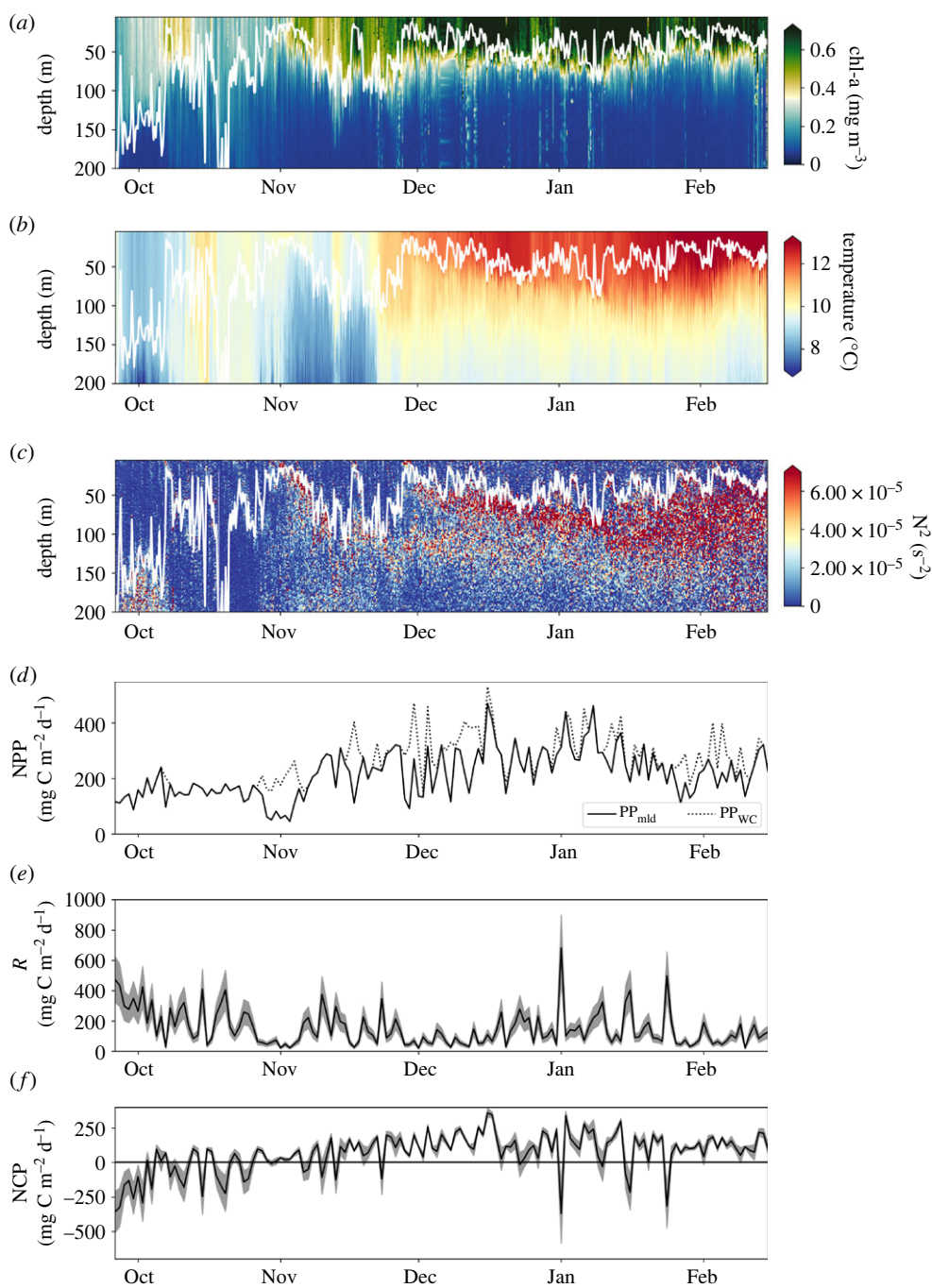
Figure 2. Sections for the SG573 glider time series from 25 September 2012 to 15 February 2013 of (*a*) chlorophyll-a concentration (mg m^{-3}), (*b*) temperature (°C) and (*c*) Brunt–Väisälä frequency (N^2; s^{-2}) used as an index for stratification. The MLD, where $\Delta T_{10m} = 0.2$°C, is overlaid in white. Time series of (*d*) modelled net primary production (NPP; mg C m^{-2} d^{-1}) integrated over the MLD (PP$_{mld}$) and the water column (PP$_{wc}$), (*e*) mean modelled respiration (R; mg C m^{-2} d^{-1}) ± standard mean error and (f) mean net community production (NCP; mg C m^{-2} d^{-1}) ± s.e. Adapted from Swart *et al.* [30] and Thomalla *et al.* [31].

phytoplankton, with rapid mixed layer eddy-driven restratification favouring productivity and allowing relatively short (1–7 days) blooms to develop earlier on in the season [30,49]. An important contribution of this work is that it provides observational evidence of the rapid

response of phytoplankton to relatively short (2–3 days) changes in the stratification induced by meso- to submesoscale processes during the spring-to-summer transition period.

A more spatially homogeneous bloom is observed in summer [30], where the dominant scale of variability in surface chlorophyll-a was monthly, but a second significant mode of variability occurred at approximately 10-day scales comparable to the physical variables of sea surface temperature and MLD [55]. Enhanced stratification from extensive warming limited the deepening of the MLD, which remained highly variable at intraseasonal time scales, fluctuating around a threshold of approximately 40 m. These MLD variations appeared to be driven by fluctuations in the wind stress from synoptic storms that undergo a rapid recovery to shallow, high light environments through feature driven buoyancy stratification [30]. Swart *et al.* [30] proposed that the observed variability of the mixed layer regulated both light and iron to the upper ocean at appropriate time scales for phytoplankton growth, thereby sustaining the bloom for an extended period through to late summer. These findings were corroborated by rates of NCP that were highly variable but generally positive throughout January and February (figure 2*f*) implying a sufficient iron source to support net autotrophy well into summer [62]. Highly variable rates of NCP were at similar time scales as the wind events that drive the MLD deepening [30,55], coinciding with peaks in respiration when exceeding the critical depth ([31]; figure 2*e*,*f*). These results support the likelihood of event scale regulation of iron and light at appropriate intervals to support sustained net autotrophy well into summer [30,53,54].

Despite the compelling evidence that these studies provide in support of the role of sub-seasonal adjustments in light and iron for enhanced growth, they do not explicitly investigate seasonal variability in iron availability. With the use of passive chlorophyll-a fluorescence on gliders, a study by Ryan-Keogh and Thomalla [63] used the degree of non-photochemical quenching (NPQ) (a decrease in measured fluorescence from the dissipation of excess energy as heat under high light conditions [64]) to derive a photophysiological indicator of iron stress. Specifically, the irradiance-normalized slope of NPQ (α_{NPQ}) acts as a proxy for iron limitation, with higher values associated with greater iron stress (electronic supplementary material, figure S2a). This proxy allows the system to be addressed at the full range of scales appropriate to the dynamics of nutrient supply and demand. The time series showed a seasonal increase in α_{NPQ} in spring, consistent with a shoaling of the MLD and an anticipated increase in iron limitation following biological utilization (electronic supplementary material, figure S2a). In summer, there was a 24% increase in α_{NPQ} variability, considered to be primarily driven by MLD. Although a direct correlation was poor ($r^2 = 0.22$), this was not unexpected given the variable response of phytoplankton to changes in the MLD [52,54]. Similar weak linear correlations were observed between physical variables and chlorophyll-a in Swart *et al.* [30] and Little *et al.* [55], however, when performing a series of correlations using rolling means (2–12 days), the correlation coefficients increased to 0.64 at an approximately 10-day window (electronic supplementary material, figure S2b). Since the dominant scales of variability of summer α_{NPQ} are coincident with the physical drivers of MLD variability, event-scale entrainment of iron is considered a key contributor to the sustained summer blooms of low SCR characteristic of the SAZ (figure 1*c*).

Together, these results emphasize the importance of fine-scale dynamics in dictating the characteristics of the seasonal cycle by driving both iron and light supply [65]. The insights gained from this body of work highlight the value of high resolution, sustained observations and their integration with biogeochemical models for targeting processes otherwise unresolvable with ship-board measurements, particularly in the remote Southern Ocean.

(b) Insights from BGC-Argo and the Southern Ocean carbon and climate observations and modelling project

Next, we highlight insights gained from another Southern Ocean programme that uses autonomous underwater vehicles, specifically profiling floats. BGC-Argo is an extension of the Argo Program to include biogeochemical observations and subsequent products for investigating

the impact of global change on biogeochemical cycles and ecosystems (https://biogeochemical-argo.org/). As with gliders, profiling floats equipped with appropriate sensors allow for an investigation of the coupling between ocean physics and biogeochemistry at scales that can address the seasonal cycle. These include approximations of NCP (e.g. [66,67]), carbon export [68] and phenology [69], all of which contribute towards a more constrained understanding of the BCP. SOCCOM is a multi-institutional US based program that uses a large fleet of BGC-Argo deployments (approx. 200) focused specifically on unlocking the mysteries of the Southern Ocean by expanding the spatial, temporal and vertical observational coverage of biogeochemical properties in this data sparse region (https://soccom.princeton.edu/). A recent SOCCOM publication by Li *et al.* [70] explored the impact of mixed-layer dynamics on productivity over intra-seasonal, seasonal and interannual time scales. Specifically, they correlated NCP anomalies with physical parameters (i.e. MLD and mean mixed layer PAR) to examine the impact of transient mixed-layer adjustments. Results reveal that the impact of mixed-layer dynamics on NCP is a function of timescales. On intraseasonal time scales, MLD and NCP are anticorrelated with NCP increasing with a shoaling of the mixed layer above the critical depth, primarily in winter and spring when iron is less likely to be limiting. In summer and autumn (when the MLD is typically shallower than the critical depth), the correlations are varied (both positive and negative) reflecting the complex interplay of light, iron and grazing (see also [52,54,71]). On seasonal timescales, NCP is primarily controlled by light availability, which is strongly influenced by winter mixing and the seasonal shoaling of the MLD in spring/summer (see also [31]), whereas on interannual timescales, NCP was weakly correlated to MLD and mean mixed layer PAR, but only in regions characterized by deep mixed layers (i.e. the subantarctic Pacific and Indian sectors in winter and spring). Their interannual investigation showed no correlation between deep winter mixing and productivity in the subsequent growing season, as has been suggested in other studies (e.g. [72,73]). Another recent study by Prend *et al.* [74] used BGC-Argo floats in conjunction with satellite ocean colour to investigate the dominant scales of variability of chlorophyll-a. Their study used three floats deployed near the Kerguelen Plateau by the Southern Ocean and Climate Field Studies with Innovative Tools project (http://soclim.com/), selected specifically as these floats have a higher sampling resolution (2–4 days) than standard biogeochemical Argo floats (10-day cycle). Results confirm that sub-seasonal variability in surface chlorophyll-a is correlated with water column integrated biomass ($R = 0.81$), such that high frequency adjustments in response to episodic mixing likely reflect a growth response in biomass rather than dilution. As was the case with satellite estimates of surface chlorophyll-a, the BGC-Argo floats reveal that interannual variability of water column integrated biomass was dominated by the sub-seasonal component, which suggests that inter annual adjustments in chlorophyll-a are related to event scale forcing [74].

(c) Insights from Southern Ocean time series

Here, we present a final example of insights gained from the SOTS mooring observatory (https://imos.org.au/facilities/deepwatermoorings/sots), an Australian contribution to the international OceanSITES global network of time-series observations. The necessity for high frequency observations sustained over many years to adequately characterize the Southern Ocean system and resolve long-term climate trajectories was recognized by SOTS who installed a set of automated moorings southwest of Tasmania in the SAZ. The observatory comprises several elements that include a deep ocean sediment trap mooring, a surface biogeochemistry mooring and an air-sea flux mooring measuring key processes that span a range of timescales from day–night to ocean basin decadal oscillations. A high-resolution temporal analysis of the moored sensors provides a phenology across four trophic levels, with results recognizing the role of deep mixing in driving the seasonality of production, the support of higher trophic levels, and the mediation of pelagic-benthic coupling [75]. This study emphasized the under-recognized contributions from winter and early spring phytoplankton activity to the transfer of carbon to the ocean interior, which is similar in magnitude to the global median, highlighting the

importance of the Southern Ocean BCP despite its 'high-nutrient, low chlorophyll' status [76]. The importance of mixed layer dynamics was similarly highlighted in a study by Weeding & Trull [77] that used high resolution measurements of dissolved oxygen and nitrogen to show that the large majority of NCP occurred in spring in the presence of deep mixed layers, with only small additional contributions in summer following water column stratification. By contrast, a study by Shadwick *et al*. [78] used high resolution CO_2 flux measurements covering a full annual cycle to reveal the seasonal interplay between physical and biological processes, with maximum uptake in midsummer driven by NCP. Autumn entrainment by a deepening mixed layer reduced CO_2 flux with full equilibration regained in late winter and spring when respiration and advection contribute to complete the annual cycle. Deep winter mixing and seasonal iron limitation were revealed as an important driver of the seasonal cycle of ecological succession between phytoplankton-dominated communities in summer and non-algal particles such as detritus that play a significant role in winter [79]. Of note is an autonomous system recently developed for the SOTS mooring that will observe the full seasonal cycle of iron concentrations at subnano molar concentrations shedding light on seasonal variability of iron limitation [80]. These results will complement NPQ estimates of iron stress from fluorescence which have similarly been shown by Schallenberg *et al*. [81] to be indicative of phytoplankton physiological state with respect to iron limitation.

3. Implications for different sampling scales

The Southern Ocean is characterized by the ubiquitous presence of energetic mesoscale structures (oceanic cyclonic and anticyclonic eddies) that are interspersed with a rich array of smaller-scale (submesoscale) filaments [82,83]. Overlaid on this complex ocean is a weather system that is characterized by the passage of storms that are frequent (e.g. 4–8 days [33]), immense (e.g. approx. 1000 km in diameter [84]) and intense (greater than $0.8\,N\,m^{-2}$ [85]). The last two decades of research have highlighted the importance of the interaction of these spatial dynamics with synoptic storms on dictating phytoplankton biomass and distribution, making it clear that a complete understanding of the sensitivity of the Southern Ocean to climate change requires ongoing efforts to address these important scales of variability. Failing to do so will result in incorrect estimates of the seasonal cycle, the annual mean and/or the variability of the system with implications for accurately determining the trajectory of the BCP and its sensitivity to climate change.

This argument is emphasized when subsampling a high-resolution dataset from the Southern Ocean to determine the minimum sampling frequency required to adequately quantify the seasonal characteristics of the time series. This approach was first proposed by Monteiro *et al*. [86] for a high-resolution CO_2 flux dataset from a wave glider. When similarly applied to a glider time series in the SAZ, i.e. subsampling the surface chlorophyll-a spring and summer time series (at the dominant periods of variability), the range of variability in the means is shown to increase substantially with a decrease in sampling frequency, indicative of a decrease in the likelihood of predicting the correct mean (electronic supplementary material, figure S3a,c). However, capturing the seasonal mean is not necessarily an adequate determinant of the seasonal cycle as it says little about the range of expressed variability. A comparison of the standard deviations of the subsampled time series (electronic supplementary material, figure S3b,d) shows that a poorly sampled time series could misinterpret the range of variability by as much as 25% in spring (15-day periodic subsample) and 29% in summer (22-day periodic subsample). These results (akin to those of [87] and [88]) reveal the sensitivity of the seasonal cycle of chlorophyll-a (and likely other biogeochemical variables) to the selected sampling frequency, which is related to the dominant scales of variability that are typically less than 10 days.

4. Linking phytoplankton dynamics to carbon export

Only a small fraction of the organic carbon fixed by primary production in the surface sunlit layers ultimately reaches the ocean interior [89–91], and it is uncertain what factors control the fraction

of production that is exported (export efficiency) or how effectively this material is transferred to depth (transfer efficiency) [92]. Factors that regulate phytoplankton growth (light, nutrients), particle formation and rates of sinking (aggregation, fragmentation, ballasting, senescence, grazing, viral lysis) and remineralization (microbial activity, chemical dissolution) all modify the extent to which fixed particulate organic carbon (POC) is transformed to dissolved organic carbon (DOC) and effectively exported and hence the efficiency of the BCP. These uncertainties were highlighted in a study by Henson *et al*. [27], which summarized 12 key processes that influence the climate sensitivity of export flux (that includes among others: particle fragmentation, zooplankton vertical migration, phytoplankton size effects on sinking and temperature/oxygen-dependent remineralization) and raised major concerns that ten of these key processes are currently missing from the majority of climate models. Their absence is considered to be partly due to a deficient mechanistic understanding of their complex role in export flux and/or a paucity of suitable observations (particularly at the relevant time and space scales) necessary to derive effective model parameterizations or validate model outputs.

Despite the complex interactions that determine the fraction of production being exported, we anticipate that since primary production, as the input to the BCP, is dominated by sub-seasonal scales of variability, it follows that the magnitude and efficiency of the BCP may be susceptible to similar scales of variability (as proposed in Henson *et al*. [93] and Giering *et al*. [94]). Indeed, Resplandy *et al*. [95] used a submesoscale permitting biophysical model to quantify the impact of small-scale physical carbon pumps and concluded that eddy-driven subduction hot spots and heterogeneities in the mixed layer at small spatial scales play a critical role in exporting carbon. However, assessing carbon export at these scales using conventional methods (e.g. ships and sediment traps) poses significant challenges, highlighting the need for innovative approaches that can resolve particle flux at high frequency.

(a) Estimating carbon export from optical sensors on autonomous platforms

When mounted on autonomous platforms, optical sensors of particle backscatter are able to provide estimates of the vertically resolved and time-varying fields needed to approximate small particle POC flux driven by mixed layer variations (e.g. [68,96]), subducted POC flux associated with small-scale ocean features (e.g. [97]), large particle aggregate flux [98], transfer efficiency [99] and fragmentation rates [100]. Results from the application of these approaches are beginning to reveal substantial regional and temporal variability in the magnitude of flux and its attenuation.

As far back as 2002, Bishop *et al*. [101] used Carbon Explorer [102] floats to highlight the link between production and export with a two- to sixfold increase in carbon export to 100 m observed in response to 'in patch' enhanced production from the effects of iron fertilization during the Southern Ocean Iron Experiment. More recently, Llort *et al*. [97] identified large variability in carbon export from BGC-Argo profiles caused by subduction events that were associated with regions of high eddy kinetic energy associated with meso and submesoscale eddies and jets. Moreau *et al*. [103] assessed patterns in the fate of phytoplankton blooms in the sea ice zone of the Weddell Sea and Indian Ocean sector (using 7 BGC-Argo floats) and revealed distinct seasonality in the two dominant loss terms of sinking flux (10%) and grazing (90%). Giddy *et al*. [73], used both gliders and floats in the Northeast Weddell Gyre to reveal distinct interannual differences in bloom characteristics (amplitude and duration), export rates and transfer efficiency. Notably, despite large interannual variability in NPP and export at 100 m, the export at 170 m was similar between two years, highlighting interannual differences in flux attenuation and export efficiency attributed to community composition, grazing and water column density structure (Giddy *et al*. [73]). Both seasonal and intra-seasonal variability in POC flux magnitude and efficiency was similarly observed in a four-month deployment of multiple gliders by the GOCART project (Gauging Ocean organic Carbon Attenuation using Robotic Technologies) downstream of South Georgia [99]. Here export efficiencies were high prior to the bloom peak (implying minimal heterotrophic consumption) but transfer efficiency was low, while during the post peak phase export flux decreased with a concomitant increase in transfer efficiency to the upper mesopelagic

11

royalsocietypublishing.org/journal/rsta   *Phil. Trans. R. Soc. A* **381**: 20220068

but a decrease in the lower mesopelagic. Notably, the proportion of primary production to reach 100 m below the export depth varied from 5 to 30% in the space of a week, confirming that carbon flux (its export and transfer efficiency) is highly episodic. These results highlight that flux attenuation varies seasonally, intra-seasonally and with depth, which is contrary to typical assumptions that are applied when extrapolating data to the global scale (e.g. [13]). Indeed, assuming time-invariance by applying a cruise-period mean export and transfer efficiency to the cruise integrated NPP resulted in an underestimate of export and sequestration flux by 49% and 45%, respectively [99].

These insights highlight the magnitude and characteristics of temporal variability in export flux and attenuation which would be impossible to achieve with shipboard campaigns alone. However, despite the obvious advantages of autonomously derived particle flux data, we nevertheless remain unable to identify all the underlying processes driving the observed variability. This is because organic matter export to the ocean's interior is governed by a complex interplay of mechanisms, the effects of which may be synergistic or antagonistic and highly variable both spatially (regionally and with depth) and temporally (from daily to seasonal and inter-annual). Ongoing technological developments, such as those that incorporate camera systems onto autonomous vehicles (e.g. [104]), have the potential to expand our understanding of this complex interplay, as do projects such as COMICS [105] and EXPORTS [106] that take a multidisciplinary approach to observing the BCP.

5. Closing the gap between fine-scales and long-term trends: future recommendations

The Southern Ocean accounts for most of the uncertainty in global Earth System Model (electronic supplementary material) estimates of both contemporary and end of century projections [107–110], with wide intermodel spread between electronic supplementary material and observations that highlight major uncertainties in our ability to accurately represent biophysical mechanisms [2,110]. This highlights the essential need for new approaches to the development of model constraints and low uncertainty global carbon budgets. Although the majority of electronic supplementary material are able to capture the basic large-scale distribution of phytoplankton (when compared with satellite observations) [111], they are not able to adequately resolve the timing and magnitude of the Southern Ocean seasonal cycle (e.g. [112–114]). These inaccuracies highlight a lack of understanding of key biogeochemical processes and the scales at which climate and biogeochemistry are linked [115], diminishing our confidence in their long-term projections. Two of the major sources of this uncertainty lies in biases that arise from incorrect parameterization of processes such as those that reflect the functional aspects of primary production and carbon export in the Southern Ocean and/or not resolving the appropriate scales of dynamics in physical–biological coupling (mesoscale and submesoscale). Insights from autonomous platforms highlight the characteristics of variability (both spatially and temporally) in the BCP (from carbon production to its export and transfer efficiency), but what is being observed in the ocean is not being adequately translated into models, highlighting the need to incorporate these findings into our conceptual understanding of the BCP, and hence into new model developments. Accurate parameterizations of phytoplankton physiology and carbon export efficiency are also hindered by our current state of conceptual understanding, limited observational data for model evaluation, and computational expense for extensive model sensitivity experiments [116]. For example, although substantial progress has been made in understanding the range of Southern Ocean iron supply mechanisms and biogeochemical cycling processes that act to govern contemporary primary production [117,118], there is an ongoing need to improve iron parameterizations in models [12,119]. There is also a need to focus research efforts on zooplankton-mediated carbon flux and improved representation of their key role in models [27,120]. Another recognized gap is an incomplete understanding of how global ocean change will affect phytoplankton and their grazers, with recommendations to upscale laboratory studies

to field experiments [121] to yield insights into trophic level responses to projected future oceanic conditions [116].

The emphasis on understanding fine-scale dynamics, and adequately parameterizing them in global climate models, has gained traction over the years and is now at the forefront of Southern Ocean research. For example, two modelling studies by Nicholson *et al*. [118,122] support the argument (emerging in particular for the SAZ) that in addition to deep winter entrainment and recycling [72], intermittent storm-driven mixing plays an important role in extending the duration of summertime production through event scale entrainment. The first [122], represents the mean characteristics of MLD perturbations in a one-dimensional biogeochemical model using a high-resolution SAZ glider deployment to reflect the impact of summer wind events. The prolonged summer bloom was only possible to emulate when incorporating a sub-seasonal iron supply mechanism through storm driven mixing and stronger diffusivities beneath the surface mixing layer (electronic supplementary material, figure S4). A second follow up study [118], used an idealized eddy-resolving physical-biogeochemical model with seasonal buoyancy forcing and zonal winds overlaid by storms to simulate seasonal and intraseasonal iron supply pathways. It showed that eddy-driven advection can contribute in equal proportions to seasonal surface iron supplies as winter convection. Further, Nicholson *et al*. [118] confirm that in summer, storms enhance both the diffusive and advective supply of iron in support of increased primary production (by 20%), particularly over regions of strong ocean fronts (electronic supplementary material, figure S5). Similarly, Uchida *et al*. [123] ran a numerical simulation at submesoscale permitting resolution forced with a realistic seasonal cycle and showed that eddy transport of iron across the base of the mixed layer provides a crucial supply of iron in support of enhanced primary production (that overcompensates for any loss due to eddy subduction) in the open Southern Ocean.

The important role of fine-scale variability in dictating the characteristics of the Southern Ocean seasonal cycle was also highlighted in a recent publication by Prend *et al*. [74] that applied a time-series decomposition of satellite chlorophyll-a to highlight distinct regional differences in the dominant timescales of chlorophyll-a variability (electronic supplementary material, figure S6). Non-seasonal variability was shown to dominate most parts of the Southern Ocean (outside of the subtropics), reflecting sub-seasonal fluctuations over small spatial scales (approx. 50–150 km). Their results (corroborated by water column integrated chlorophyll-a from three BGC-Argo floats off Kerguelen) suggest that sub-seasonal variability exceeds inter-annual variability and as a result, year-to-year variations of annual mean chlorophyll-a primarily reflect high frequency events related to localized forcing such as storms and eddies, rather than low-frequency climate modes (such as the Southern Annular Mode). This is because the magnitude of the seasonally integrated bloom is dictated by the sum of intermittent pulses occurring at approximately weekly timescales (as hypothesized for the light green regions in figure 1*c* [29]). The impact of this understanding is that changes in annual mean chlorophyll-a (and by association the BCP) are tied to forcings that drive sub-seasonal fluctuations [74], such that the impact of climate variability will likely be reflected in localized responses to adjustments in wind [124–126] and/or eddy activity [127,128]. That said, although the degree to which large-scale atmospheric variability drives intense short-term wind events remains unclear [129,130], a study by Hell *et al*. [131] statistically explored variability in the SAM (i.e. large-scale modes of atmospheric variability) with short-term surface wind and stress. Results from time-varying 5-day probability density functions confirm that the first two modes of wind (72% of total wind variance) and stress (74% of total stress variance) are highly correlated ($R = 0.82$) with the SAM. The implication of these findings is that large-scale low-frequency climate modes may still be considered important in determining the trajectory of the BCP, although indirectly through their influence on high frequency storm intensity. Notably, if storm driven interactions with the MLD are the primary driver of the characteristics of the seasonal bloom (and inter-annual variability), then the regional nature and long-term trends in storm characteristics may be an important influence in the future role of the Southern Ocean in the carbon-climate system [86]. It is thus necessary that we work towards the paramaterization of fine-scale (sub-grid) dynamics

in earth system models at a low computing overhead for improved confidence in climate trajectories.

Satellite remote sensing of ocean colour is the only observational capability that can provide synoptic views of upper ocean phytoplankton characteristics at high spatial and temporal resolution (approx. 1 km, daily) and high temporal extent (global scales, for years to decades). In many cases, these are the only systematic observations available for chronically under-sampled marine systems such as the Southern Ocean. It is thus necessary that we maximize the value of remote sensing observations for this globally critical region by developing ecosystem-appropriate, well characterized ocean colour products. Phytoplankton cell size and elemental stoichiometry impose fundamental constraints on growth rates, food web structure and the biogeochemical cycling of carbon [132]. Despite the large variability evident across projected climate driven shifts in phytoplankton community composition [133] a reduction in dominant size and a shift away from diatoms is considered a particularly strong driver of projected decreases in export [134]. As such, a primary goal of the endeavour to maximize outputs from remote sensing observations is to provide information on the phytoplankton community (e.g. size structure and taxonomic composition), which translates into carbon export. This was achieved in a study by Siegel *et al*. [135] that combined satellite-based estimates of primary production [136] and particle size distribution from backscatter [137] with a food-web model for global assessments of sinking carbon export. This approach was able to effectively capture seasonal cycles in carbon export and assess drivers of interannual variability (equatorward of 50°) providing a diagnostic tool for addressing time and space variability in the processes driving carbon export [135]. That said, the fidelity of this approach is highly dependent on the ability of remote sensing algorithms to accurately determine primary production and particle size. Although some ocean colour algorithms can accurately derive chlorophyll-a for the Southern Ocean [138], the simple lack of *in situ* data means that satellite product retrieval algorithms are typically not well tailored to the Southern Ocean, and their performance is generally unreliable or even largely unknown [139]. Concerning optical products in particular, evidence suggests that the unique photophysiological characteristics of Southern Ocean phytoplankton (e.g. cellular adjustments to light and iron stress) may play a large role in determining their distinct characteristics of absorption [140]. Additionally, particulate backscatter in the Southern Ocean has been observed to imply regionally unusual particulate assemblage characteristics [141]. As such, Inherent Optical Property retrievals from standard ocean colour algorithms cannot be used with confidence in the Southern Ocean when parameterized primarily with low-latitude bio-optical datasets whose properties differ from those of the Southern Ocean [75]. These shortcomings are propagated when deriving biogeochemical products (e.g. size structure [142], carbon content [143,144] and phytoplankton functional type [145,146]), for which results are typically extremely variable, with large disagreement between products. These issues highlight the need for ongoing efforts to apply emerging techniques to derive a causal understanding of the unique characteristics of Southern Ocean bio-optics towards the optimization and development of regionally robust information from ocean colour that will allow new insight into event, seasonal, inter-annual and long-term variability in ecosystem physical drivers and their biogeochemical response.

Despite their obvious spatial and temporal advantages, remotely detected water-leaving radiances emanate from only the first optical depth and give little quantitative information about the vertical structure of the water column. Arguably the frontier in ocean observation is sustained spatial sampling of the subsurface ocean [147] by autonomous platforms (e.g. gliders and floats) that have the capacity to address fine-scale variability in physical drivers and biological response (relating to both productivity and export). Gliders and floats are able to profile the water column (0–1000 m) at high frequency to provide highly cost-effective measurements of physical structure and biogeochemistry at smaller scales, but also for sufficiently long periods to address uncertainties associated with carbon budgets at longer time scales (weeks—months). In addition, the volume of information that a single glider or BGC-float mission retrieves, can be instrumental in developing and validating statistically robust parameterizations for numerical models, which are otherwise performed with oftentimes inadequate datasets

generated from once-off or 'classical' (low spatial and/or low temporal frequency) sampling techniques. A comprehensive review by Swart *et al*. [50] summarizes a decade of mechanistic understanding gained from autonomous platforms on the role of fine-scale processes influencing mixed layer variability. In addition, there is evidence of the growing potential of these platforms to measure rates of production, respiration, carbon export, sinking fluxes and particle fragmentation [96,98,100,148,149]. Given their importance in the trajectory of ocean ecosystem understanding, it is fundamental that we continue to develop new methods and sensors for detecting biogeochemical properties from autonomous platforms.

Integrating these research approaches, i.e. ocean colour remote sensing, the network of BGC-Argo floats, glider missions and stationary moorings, is necessary for accumulating the temporal and spatial data coverage needed to improve our understanding of the Southern Ocean BCP [120]. The next challenge is to find ways of synthesizing this information (from remote sensing and autonomous platforms) from a wide range of environmental conditions and spatio-temporal scales into robust mechanistic parameterizations for global models, and/or global validation datasets for model comparisons [27].

References

1. DeVries T, Holzer M, Primeau F. 2017 Recent increase in oceanic carbon uptake driven by weaker upper-ocean overturning. *Nature* **542**, 215–218. (doi:10.1038/nature21068)
2. Friedlingstein P *et al*. 2019 Global carbon budget 2019. *Earth Syst. Sci. Data* **11**, 1783–1838. (doi:10.5194/essd-11-1783-2019)
3. Frölicher TL, Sarmiento JL, Paynter DJ, Dunne JP, Krasting JP, Winton M. 2015 Dominance of the Southern Ocean in anthropogenic carbon and heat uptake in CMIP5 models. *J. Clim.* **28**, 862–886. (doi:10.1175/JCLI-D-14-00117.1)
4. Lenton A *et al*. 2013 Sea–air CO_2 fluxes in the Southern Ocean for the period 1990–2009. *Biogeosciences* **10**, 4037–4054. (doi:10.5194/bg-10-4037-2013)
5. Takahashi T *et al*. 2009 Climatological mean and decadal change in surface ocean pCO_2, and net sea–air CO_2 flux over the global oceans. *Deep Sea Res. II* **56**, 554–577. (doi:10.1016/j.dsr2.2008.12.009)
6. Hauck J, Lenton A, Langlais C, Matear R. 2018 The fate of carbon and nutrients exported out of the Southern Ocean. *Global Biogeochem. Cycles* **32**, 1556–1573. (doi:10.1029/2018GB005977)

7. Schlitzer R. 2002 Carbon export fluxes in the Southern Ocean: results from inverse modeling and comparison with satellite-based estimates. *Deep Sea Res. Part II* **49**, 1623–1644. (doi:10.1016/S0967-0645(02)00004-8)

8. Mikaloff Fletcher SE *et al.* 2007 Inverse estimates of the oceanic sources and sinks of natural CO_2 and the implied oceanic carbon transport. *Global Biogeochem. Cycles* **21**, 1–19. (doi:10.1029/2006GB002751)

9. Gruber N *et al.* 2009 Oceanic sources, sinks, and transport of atmospheric CO_2. *Global Biogeochem. Cycles* **23**, GB1005. (doi:10.1029/2008GB003349)

10. Bopp L *et al.* 2013 Multiple stressors of ocean ecosystems in the 21st century: projections with CMIP5 models. *Biogeosciences* **10**, 6225–6245. (doi:10.5194/bg-10-6225-2013)

11. Boyd PW, Lennartz ST, Glover DM, Doney SC. 2015 Biological ramifications of climate-change-mediated oceanic multi-stressors. *Nat. Clim. Change* **5**, 71–79. (doi:10.1038/nclimate2441)

12. Kwiatkowski L *et al.* 2020 Twenty-first century ocean warming, acidification, deoxygenation, and upper-ocean nutrient and primary production decline from CMIP6 model projections. *Biogeosciences* **17**, 3439–3470. (doi:10.5194/bg-17-3439-2020)

13. Henson SA, Sanders R, Madsen E, Morris PJ, Le Moigne F, Quartly GD. 2011 A reduced estimate of the strength of the ocean's biological carbon pump. *Geophys. Res. Lett.* **38**, 1–5. (doi:10.1029/2011GL046735)

14. Palter JB, Sarmiento JL, Gnanadesikan A, Simeon J, Slater RD. 2010 Fueling export production: nutrient return pathways from the deep ocean and their dependence on the meridional overturning circulation. *Biogeosciences* **7**, 3549–3568. (doi:10.5194/bg-7-3549-2010)

15. Sarmiento JL, Gruber N, Brzezinski MA, Dunne JP. 2004 High-latitude controls of thermocline nutrients and low latitude biological productivity. *Nature* **427**, 56–60. (doi:10.1038/nature02127)

16. Sigman DM, Boyle EA. 2000 Glacial/interglacial variations in atmospheric carbon dioxide. *Nature* **407**, 859–869. (doi:10.1038/35038000)

17. Hauck J *et al.* 2015 On the Southern Ocean CO_2 uptake and the role of the biological carbon pump in the 21st century. *Global Biogeochem. Cycles* **29**, 1451–1470. (doi:10.1002/2015GB005140)

18. Krishnamurthy A, Moore JK, Mahowald N, Luo C, Doney SC, Lindsay K, Zender CS. 2009 Impacts of increasing anthropogenic soluble iron and nitrogen deposition on ocean biogeochemistry. *Global Biogeochem. Cycles* **23**, GB3016. (doi:10.1029/2008GB003440)

19. Barnes DKA. 2018 Blue carbon on polar and subpolar seabeds. In *Carbon capture, utilization and sequestration* (ed. RK Agarwal), Rijeka: IntechOpen.

20. Henley SF *et al.* 2020 Changing biogeochemistry of the southern ocean and its ecosystem implications. *Front. Mar. Sci.* **7**, 581. (doi:10.3389/fmars.2020.00581)

21. Morley SA *et al.* 2020 Global drivers on southern ocean ecosystems: changing physical environments and anthropogenic pressures in an earth system. *Front. Mar. Sci.* **7**, 547188. (doi:10.3389/fmars.2020.547188)

22. Auger M, Morrow R, Kestenare E, Sallée J-B, Cowley R. 2021 Southern Ocean in-situ temperature trends over 25 years emerge from interannual variability. *Nat. Commun.* **12**, 514. (doi:10.1038/s41467-020-20781-1)

23. Haumann FA, Gruber N, Münnich M. 2020 Sea-ice induced southern ocean subsurface warming and surface cooling in a warming climate. *AGU Adv.* **1**, e2019AV000132. (doi:10.1029/2019AV000132)

24. Sallée J-B, Pellichero V, Akhoudas C, Pauthenet E, Vignes L, Schmidtko S, Garabato AN, Sutherland P, Kuusela M. 2021 Summertime increases in upper-ocean stratification and mixed-layer depth. *Nature* **591**, 592–598. (doi:10.1038/s41586-021-03303-x)

25. Swart NC, Fyfe JC, Saenko OA, Eby M. 2014 Wind-driven changes in the ocean carbon sink. *Biogeosciences* **11**, 6107–6117. (doi:10.5194/bg-11-6107-2014)

26. Laufkötter C, John JG, Stock CA, Dunne JP. 2017 Temperature and oxygen dependence of the remineralization of organic matter. *Global Biogeochem. Cycles* **31**, 1038–1050. (doi:10.1002/2017GB005643)

27. Henson SA, Laufkötter C, Leung S, Giering SLC, Palevsky HI, Cavan EL. 2022 Uncertain response of ocean biological carbon export in a changing world. *Nat. Geosci.* **15**, 248–254. (doi:10.1038/s41561-022-00927-0)

28. IPCC. 2021 *Climate change 2021: The physical science basis. Contribution of working group I to the sixth assessment report of the intergovernmental panel on climate change*. Cambridge, UK: Cambridge University Press.

29. Thomalla SJ, Fauchereau N, Swart S, Monteiro PMS. 2011 Regional scale characteristics of the seasonal cycle of chlorophyll in the Southern Ocean. *Biogeosciences* **8**, 2849–2866. (doi:10.5194/bg-8-2849-2011)

30. Swart S, Thomalla SJ, Monteiro PMS. 2015 The seasonal cycle of mixed layer dynamics and phytoplankton biomass in the Sub-Antarctic Zone: a high-resolution glider experiment. *J. Mar. Sys.* **147**, 103–115. (doi:10.1016/j.jmarsys.2014.06.002)

31. Thomalla SJ, Racault M, Swart S, Monteiro PMS. 2015 High-resolution view of the spring bloom initiation and net community production in the Subantarctic Southern Ocean using glider data. *ICES J. Mar. Sci.* **72**, 1999–2020. (doi:10.1093/ICESJMS/FSV105)

32. Monteiro PMS, Boyd P, Bellerby R. 2011 Role of the seasonal cycle in coupling climate and carbon cycling in the Subantarctic zone. *Eos, Trans. Am. Geophys. Union* **92**, 235–236. (doi:10.1029/2011EO280007)

33. Carranza MM, Gille ST, Franks PJS, Johnson KS, Pinkel R, Girton JB. 2018 When mixed layers are not mixed. Storm-Driven mixing and bio-optical vertical gradients in mixed layers of the Southern Ocean. *J. Geophys. Res. Oceans* **123**, 7264–7289. (doi:10.1029/2018JC014416)

34. Henson SA, Cole HS, Hopkins J, Martin AP, Yool A. 2018 Detection of climate change-driven trends in phytoplankton phenology. *Global Change Biol.* **24**, e101–e111. (doi:10.1111/gcb.13886)

35. Cox PM. 2019 Emergent constraints on climate-carbon cycle feedbacks. *Curr. Clim. Change Rep.* **5**, 275–281. (doi:10.1007/S40641-019-00141-Y)

36. Boyd PW. 2002 Environmental factors controlling phytoplankton processes in the Southern Ocean. *J. Phycol.* **38**, 844–861. (doi:10.1046/j.1529-8817.2002.t01-1-01203.x)

37. Boyd P, LaRoche J, Gall M, Frew R, McKay RML. 1999 Role of iron, light, and silicate in controlling algal biomass in Subantarctic waters SE of New Zealand. *J. Geophys. Res. Oceans* **104**, 13 395–13 408. (doi:10.1029/1999JC900009)

38. Franck VM, Brzezinski MA, Coale KH, Nelson DM. 2000 Iron and silicic acid concentrations regulate Si uptake north and south of the Polar Frontal Zone in the Pacific Sector of the Southern Ocean. *Deep Sea Res. Part II* **47**, 3315–3338. (doi:10.1016/S0967-0645(00)00 070-9)

39. Nelson DM, Brzezinski MA, Sigmon DE, Franck VM. 2001 A seasonal progression of Si limitation in the Pacific sector of the Southern Ocean. *Deep Sea Res. Part II* **48**, 3973–3995. (doi:10.1016/S0967-0645(01)00076-5)

40. Tortell PD, DiTullio GR, Sigman DM, Morel FMM. 2002 CO_2 effects on taxonomic composition and nutrient utilization in an Equatorial Pacific phytoplankton assemblage. *Mar. Ecol. Prog. Ser.* **236**, 37–43. (doi:10.3354/meps236037)

41. Klein P, Lapeyre G. 2009 The oceanic vertical pump induced by mesoscale and submesoscale turbulence. *Annu. Rev. Mar. Sci.* **1**, 351–375. (doi:10.1146/annurev.marine.010908.163704)

42. McGillicuddy DJ, Anderson LA, Doney SC, Maltrud ME. 2003 Eddy-driven sources and sinks of nutrients in the upper ocean: results from a 0.1 degrees resolution model of the North Atlantic. *Global Biogeochem. Cycles* **17**, 1035. (doi:10.1029/2002gb001987)

43. McGillicuddy DJ *et al.* 2007 Eddy/wind interactions stimulate extraordinary mid-ocean plankton blooms. *Science (1979)* **316**, 1021–1026. (doi:10.1126/science.1136256)

44. Jenkins WJ. 1988 Nitrate flux into the euphotic zone near Bermuda. *Nature* **331**, 521–523. (doi:10.1038/331521a0)

45. Ferrari R, Wunsch C. 2008 Ocean circulation kinetic energy: reservoirs, sources, and sinks. *Annu. Rev. Fluid Mech.* **41**, 253–282. (doi:10.1146/annurev.fluid.40.111406.102139)

46. Lévy M, Klein P, Treguier AM. 2001 Impact of sub-mesoscale physics on production and subduction of phytoplankton in an oligotrophic regime. *J. Mar. Res.* **59**, 535–565. (https://archimer.ifremer.fr/doc/2001/publication-800.pdf)

47. Glover DM, Doney SC, Nelson NB, Wallis A. 2008 Sub-mesoscale anisotropy (fronts, eddies, and filaments) as observed near Bermuda with ocean color data. Paper presented at: 2008 Ocean Sciences Meeting. In *Proc. of the 2008 Ocean Sciences Meeting, Orlando, FL, 2–7 March 2008*, pp. 2–7. Washington, DC: AGU.

48. Lévy M, Klein P, ben Jelloul M. 2009 New production stimulated by high-frequency winds in a turbulent mesoscale eddy field. *Geophys. Res. Lett.* **36**, 1–5. (doi:10.1029/2009GL039490)

49. Mahadevan A, D'Asaro E, Lee C, Perry MJ. 2012 Eddy-driven stratification initiates north Atlantic spring phytoplankton blooms. *Science (1979)* **337**, 54 LP–54 58. (doi:10.1126/science.1218740)

50. Swart S *et al.* 2023 The Southern Ocean mixed layer and its boundary fluxes: fine-scale observational progress and future research priorities. *Phil. Trans R. Soc. A* **381**, 20220058. (doi:10.1098/rsta.2022.0058)

51. Sathyendranath S *et al.* 2019 An ocean-colour time series for use in climate studies: the experience of the ocean-colour climate change initiative (OC-CCI). *Sensors* **19**, 4285. (doi:10.3390/s19194285)

52. Fauchereau N, Tagliabue A, Bopp L, Monteiro PMS. 2011 The response of phytoplankton biomass to transient mixing events in the Southern Ocean. *Geophys. Res. Lett.* **38**, 1–6. (doi:10.1029/2011GL048498)

53. Joubert WR, Swart S, Tagliabue A, Thomalla SJ, Monteiro PMS. 2014 The sensitivity of primary productivity to intra-seasonal mixed layer variability in the sub-Antarctic Zone of the Atlantic Ocean. *Biogeosci. Dis.* **11**, 4335–4358. (doi:10.5194/bgd-11-4335-2014)

54. Carranza MM, Gille ST. 2015 Southern Ocean wind-driven entrainment enhances satellite chlorophyll-a through the summer. *J. Geophys. Res. Oceans* **120**, 304–323. (doi:10.1002/2014JC010203)

55. Little HJ, Vichi M, Thomalla SJ, Swart S. 2018 Spatial and temporal scales of chlorophyll variability using high-resolution glider data. *J. Mar. Sys.* **187**, 1–12. (https://www.science direct.com/science/article/abs/pii/S0924796317304530)

56. Taylor JR, Ferrari R. 2011 Shutdown of turbulent convection as a new criterion for the onset of spring phytoplankton blooms. *Limnol. Oceanogr.* **56**, 2293–2307. (doi:10.4319/lo.2011.56.6.2293)

57. Chiswell SM. 2011 Annual cycles and spring blooms in phytoplankton: don't abandon Sverdrup completely. *Mar. Ecol. Prog. Ser.* **443**, 39–50. (doi:10.3354/meps09453)

58. Chiswell SM, Bradford-Grieve J, Hadfield MG, Kennan SC. 2013 Climatology of surface chlorophyll a, autumn-winter and spring blooms in the southwest Pacific Ocean. *J. Geophys. Res. Oceans* **118**, 1003–1018. (doi:10.1002/jgrc.20088)

59. du Plessis M, Swart S, Ansorge IJ, Mahadevan A. 2017 Submesoscale processes promote seasonal restratification in the Subantarctic Ocean. *J. Geophys. Res. Oceans* **122**, 2960–2975. (doi:10.1002/2016JC012494)

60. du Plessis M, Swart S, Ansorge IJ, Mahadevan A, Thompson AF. 2019 Southern Ocean seasonal restratification delayed by submesoscale wind–front interactions. *J. Phys. Oceanogr.* **49**, 1035–1053. (doi:10.1175/JPO-D-18-0136.1)

61. Mahadevan A, Tandon A, Ferrari R. 2010 Rapid changes in mixed layer stratification driven by submesoscale instabilities and winds. *J. Geophys. Res. Oceans* **115**, C03017. (doi:10.1029/2008JC005203)

62. Cassar N *et al.* 2011 The influence of iron and light on net community production in the Subantarctic and polar frontal zones. *Biogeosciences* **8**, 227–237. (doi:10.5194/bg-8-227-2011)

63. Ryan-Keogh TJ, Thomalla SJ. 2020 Deriving a proxy for iron limitation from chlorophyll fluorescence on buoyancy gliders. *Front. Mar. Sci.* **7**, 275. (doi:10.3389/fmars.2020.00275)

64. van Leeuwe MA, Stefels J. 2007 Photosynthetic responses in Phaeocystis Antarctica towards varying light and iron conditions. *Biogeochemistry* **83**, 61–70. (doi:10.1007/s10533-007-9083-5)

65. Ryan-Keogh TJ, Thomalla SJ, Mtshali TN, van Horsten NR, Little HJ. 2018 Seasonal development of iron limitation in the sub-Antarctic zone. *Biogeosciences* **15**, 4647–4660. (doi:10.5194/bg-15-4647-2018)

66. Alkire MB *et al.* 2012 Estimates of net community production and export using high-resolution, Lagrangian measurements of O_2, NO_{3-}, and POC through the evolution of a spring diatom bloom in the North Atlantic. *Deep Sea Res. Part I* **64**, 157–174. (doi:10.1016/j.dsr.2012.01.012)

67. Plant JN, Johnson KS, Sakamoto CM, Jannasch HW, Coletti LJ, Riser SC, Swift DD. 2016 Net community production at Ocean Station Papa observed with nitrate and oxygen sensors on profiling floats. *Global Biogeochem. Cycles* **30**, 859–879. (doi:10.1002/2015GB005349)

68. Dall'Olmo G, Mork KA. 2014 Carbon export by small particles in the Norwegian Sea. *Geophys. Res. Lett.* **41**, 2921–2927. (doi:10.1002/2014GL059244)

69. Boss E, Behrenfeld M. 2010 In situ evaluation of the initiation of the North Atlantic phytoplankton bloom. *Geophys. Res. Lett.* **37**, L18603. (doi:10.1029/2010GL044174)

70. Li Z, Lozier MS, Cassar N. 2021 Linking Southern Ocean mixed-layer dynamics to net community production on various timescales. *J. Geophys. Res. Oceans* **126**, e2021JC017537. (doi:10.1029/2021JC017537)

71. Llort J, Lévy M, Sallée JB, Tagliabue A. 2019 Nonmonotonic response of primary production and export to changes in mixed-layer depth in the Southern Ocean. *Geophys. Res. Lett.* **46**, 3368–3377. (doi:10.1029/2018GL081788)

72. Tagliabue A, Sallée JB, Bowie AR, Lévy M, Swart S, Boyd PW. 2014 Surface-water iron supplies in the Southern Ocean sustained by deep winter mixing. *Nat. Geosci.* **7**, 314–320. (doi:10.1038/ngeo2101)

73. Giddy I, Nicholson S, Queste BY, Thomalla S, Swart S. 2011 Sea-ice impacts inter-annual variability in phytoplankton phenology and carbon export in the Weddell Sea. *Geophys. Res. Lett.* **38**. (doi:10.1002/essoar.10508727.1)

74. Prend CJ, Keerthi MG, Lévy M, Aumont O, Gille ST, Talley LD. 2022 Sub-seasonal forcing drives year-to-year variations of southern ocean primary productivity. *Global Biogeochem. Cycles* **36**, e2022GB007329. (doi:10.1029/2022GB007329)

75. Trull TW, Jansen P, Schulz E, Weeding B, Davies DM, Bray SG. 2019 Autonomous multi-trophic observations of productivity and export at the Australian Southern Ocean Time Series (SOTS) reveal sequential mechanisms of physical-biological coupling. *Front. Mar. Sci.* **6**, 525. (doi:10.3389/fmars.2019.00525)

76. Trull TW, Bray SG, Manganini SJ, Honjo S, François R. 2001 Moored sediment trap measurements of carbon export in the Subantarctic and polar frontal zones of the Southern Ocean, south of Australia. *J. Geophys. Res. Oceans* **106**, 31 489–31 509. (doi:10.1029/2000JC000308)

77. Weeding B, Trull TW. 2014 Hourly oxygen and total gas tension measurements at the Southern Ocean time series site reveal winter ventilation and spring net community production. *J. Geophys. Res. Oceans* **119**, 348–358. (doi:10.1002/2013JC009302)

78. Shadwick EH, Tilbrook B, Cassar N, Trull TW, Rintoul SR. 2015 Summertime physical and biological controls on O_2 and CO_2 in the Australian sector of the Southern Ocean. *J. Mar. Sys.* **147**, 21–28. (doi:10.1016/j.jmarsys.2013.12.008)

79. Schallenberg C, Harley JW, Jansen P, Davies DM, Trull TW. 2019 Multi-year observations of fluorescence and backscatter at the Southern Ocean time series (SOTS) shed light on two distinct seasonal bio-optical regimes. *Front. Mar. Sci.* **6**, 595. (doi:10.3389/fmars.2019.00595)

80. van der Merwe P, Trull TW, Goodwin T, Jansen P, Bowie A. 2019 The autonomous clean environmental (ACE) sampler: a trace-metal clean seawater sampler suitable for open-ocean time-series applications. *Limnol. Oceanogr. Methods* **17**, 490–504. (doi:10.1002/lom3.10327)

81. Schallenberg C, Strzepek RF, Schuback N, Clementson LA, Boyd PW, Trull TW. 2020 Diel quenching of Southern Ocean phytoplankton fluorescence is related to iron limitation. *Biogeosciences* **17**, 793–812. (doi:10.5194/bg-17-793-2020)

82. Su Z, Wang J, Klein P, Thompson AF, Menemenlis D. 2018 Ocean submesoscales as a key component of the global heat budget. *Nat. Commun.* **9**, 775. (doi:10.1038/s41467-018-02983-w)

83. Hewitt H, Fox-Kemper B, Pearson B, Roberts M, Klocke D. 2022 The small scales of the ocean may hold the key to surprises. *Nat. Clim. Change* **12**, 496–499. (doi:10.1038/s41558-022-01386-6)

84. Patoux J, Yuan X, Li C. 2009 Satellite-based midlatitude cyclone statistics over the Southern Ocean: 1. Scatterometer-derived pressure fields and storm tracking. *J. Geophys. Res. Atmos.* **114**, D04105. (doi:10.1029/2008JD010873)

85. Yuan X. 2004 High-wind-speed evaluation in the Southern Ocean. *J. Geophys. Res. Atmos.* **109**, 1–10. (doi:10.1029/2003JD004179)

86. Monteiro PMS, Gregor L, Lévy M, Maenner S, Sabine CL, Swart S. 2015 Intraseasonal variability linked to sampling alias in air-sea CO_2 fluxes in the Southern Ocean. *Geophys. Res. Lett.* **42**, 8507–8514. (doi:10.1002/2015GL066009)

87. Hales B, Takahashi T. 2004 High-resolution biogeochemical investigation of the Ross Sea, Antarctica, during the AESOPS (U. S. JGOFS) Program. *Global Biogeochem. Cycles* **18**, 1–24. (doi:10.1029/2003GB002165)

88. Kaufman DE, Friedrichs MAM, Hemmings JCP, Smith Jr WO. 2018 Assimilating bio-optical glider data during a phytoplankton bloom in the southern Ross Sea. *Biogeosciences* **15**, 73–90. (doi:10.5194/bg-15-73-2018)

89. Martin JH, Knauer GA, Karl DM, Broenkow WW. 1987 VERTEX: carbon cycling in the northeast Pacific. *Deep Sea Research Part A. Oceanogr. Res. Papers* **34**, 267–285. (doi:10.1016/0198-0149(87)90086-0)

90. Steinberg DK, van Mooy BAS, Buesseler KO, Boyd PW, Kobari T, Karl DM. 2008 Bacterial vs. zooplankton control of sinking particle flux in the ocean's twilight zone. *Limnol. Oceanogr.* **53**, 1327–1338. (doi:10.4319/lo.2008.53.4.1327)

91. Giering SLC *et al.* 2014 Reconciliation of the carbon budget in the ocean's twilight zone. *Nature* **507**, 480–483. (doi:10.1038/nature13123)

92. Cavan EL, le Moigne FAC, Poulton AJ, Tarling GA, Ward P, Daniels CJ, Fragoso GM, Sanders RJ. 2015 Attenuation of particulate organic carbon flux in the Scotia Sea, Southern Ocean, is controlled by zooplankton fecal pellets. *Geophys. Res. Lett.* **42**, 821–830. (doi:10.1002/2014GL062744)

93. Henson SA, Yool A, Sanders R. 2015 Variability in efficiency of particulate organic carbon export: a model study. *Global Biogeochem. Cycles* **29**, 33–45. (doi:10.1002/2014GB004965)

94. Giering SLC, Sanders R, Martin AP, Henson SA, Riley JS, Marsay CM, Johns DG. 2017 Particle flux in the oceans: challenging the steady state assumption. *Global Biogeochem. Cycles* **31**, 159–171. (doi:10.1002/2016GB005424)

95. Resplandy L, Lévy M, McGillicuddy Jr DJ. 2019 Effects of Eddy-Driven subduction on ocean biological carbon pump. *Global Biogeochem. Cycles* **33**, 1071–1084. (doi:10.1029/2018GB006125)

96. Bol R, Henson SA, Rumyantseva A, Briggs N. 2018 High-frequency variability of small-particle carbon export flux in the Northeast Atlantic. *Global Biogeochem. Cycles* **32**, 1803–1814. (doi:10.1029/2018GB005963)

97. Llort J, Langlais C, Matear R, Moreau S, Lenton A, Strutton PG. 2018 Evaluating Southern Ocean carbon eddy-pump from biogeochemical-argo floats. *J. Geophys. Res. Oceans* **123**, 971–984. (doi:10.1002/2017JC012861)

98. Briggs N, Perry MJ, Cetinić I, Lee C, D'Asaro E, Gray AM, Rehm E. 2011 High-resolution observations of aggregate flux during a sub-polar North Atlantic spring bloom. *Deep Sea Res. Oceanogr. Res. Pap.* **58**, 1031–1039. (doi:10.1016/j.dsr.2011.07.007)

99. Henson SA, Briggs N, Carvalho F, Manno C, Mignot A, Thomalla S. 2023 A seasonal transition in biological carbon pump efficiency in the northern Scotia Sea, Southern Ocean. *Deep Sea Res. Part II* **208**, 105274. (doi:10.1016/j.dsr2.2023.105274)

100. Briggs N, Dall'Olmo G, Claustre H. 2020 Major role of particle fragmentation in regulating biological sequestration of CO_2 by the oceans. *Science (1979)* **367**, 791 LP–791793. (doi:10.1126/science.aay1790)

101. Bishop JKB, Wood TJ, Davis RE, Sherman JT. 2004 Robotic observations of enhanced carbon biomass and export at 55°s during SOFeX. *Science (1979)* **304**, 417–420. (doi:10.1126/science.1087717)

102. Bishop JKB, Davis RE, Sherman JT. 2002 Robotic observations of dust storm enhancement of carbon biomass in the North Pacific. *Science (1979)* **298**, 817–821. (doi:10.1126/science.1074961)

103. Moreau S, Boyd PW, Strutton PG. 2020 Remote assessment of the fate of phytoplankton in the Southern Ocean sea-ice zone. *Nat. Commun.* **11**, 3108. (doi:10.1038/s41467-020-16931-0)

104. Lombard F *et al.* 2019 Globally consistent quantitative observations of planktonic ecosystems. *Front. Mar. Sci.* **6**, 196. (doi:10.3389/fmars.2019.00196)

105. Sanders RJ *et al.* 2016 Controls over ocean mesopelagic interior carbon storage (COMICS): fieldwork, synthesis, and modeling efforts. *Front. Mar. Sci.* **3**, 136. (doi:10.3389/fmars.2016.00136)

106. Siegel DA *et al.* 2016 Prediction of the export and fate of global ocean net primary production: The EXPORTS science plan. *Front. Mar. Sci.* **3**, 22. (doi:10.3389/fmars.2016.00022)

107. Gregor L, Kok S, Monteiro PMS. 2018 Interannual drivers of the seasonal cycle of CO_2 in the Southern Ocean. *Biogeosciences* **15**, 2361–2378. (doi:10.5194/bg-15-2361-2018)

108. Gregor L, Lebehot AD, Kok S, Scheel Monteiro PM. 2019 A comparative assessment of the uncertainties of global surface ocean CO_2 estimates using a machine-learning ensemble (CSIR-ML6 version 2019a) – have we hit the wall? *Geosci. Model Dev.* **12**, 5113–5136. (doi:10.5194/gmd-12-5113-2019)

109. Mongwe NP, Chang N, Monteiro PMS. 2016 The seasonal cycle as a mode to diagnose biases in modelled CO_2 fluxes in the Southern Ocean. *Ocean Model (Oxf)* **106**, 90–103. (doi:10.1016/j.ocemod.2016.09.006)

110. Mongwe NP, Vichi M, Monteiro PMS. 2018 The seasonal cycle of pCO_2 and CO_2 fluxes in the Southern Ocean: diagnosing anomalies in CMIP5 Earth system models. *Biogeosciences* **15**, 2851–2872. (doi:10.5194/bg-15-2851-2018)

111. McKiver WJ, Vichi M, Lovato T, Storto A, Masina S. 2015 Impact of increased grid resolution on global marine biogeochemistry. *J. Mar. Sys.* **147**, 153–168. (doi:10.1016/j.jmarsys.2014.10.003)

112. Vichi M, Masina S. 2009 Skill assessment of the PELAGOS global ocean biogeochemistry model over the period 1980–2000. *Biogeosciences* **6**, 2333–2353. (doi:10.5194/bg-6-2333-2009)

113. Doney SC, Lima I, Moore JK, Lindsay K, Behrenfeld MJ, Westberry TK, Mahowald N, Glover DM, Takahashi T. 2009 Skill metrics for confronting global upper ocean ecosystem-biogeochemistry models against field and remote sensing data. *J. Mar. Sys.* **76**, 95–112. (doi:10.1016/j.jmarsys.2008.05.015)

114. Steinacher M *et al.* 2010 Projected 21st century decrease in marine productivity: a multi-model analysis. *Biogeosciences* **7**, 979–1005. (doi:10.5194/bg-7-979-2010)

115. Swart S *et al.* 2012 Southern ocean seasonal cycle experiment 2012: seasonal scale climate and carbon cycle links. *S. Afr. J. Sci.* **108**, 3–5. (doi:10.4102/sajs.v108i3/4.1089)

116. Boyd PW, Doney SC, Eggins S, Ellwood MJ, Fourquez M, Nunn BL, Strzepek R, Timmins-Schiffman E. 2022 Transitioning global change experiments on Southern Ocean phytoplankton from lab to field settings: Insights and challenges. *Limnol. Oceanogr.* **67**, 1911–1930. (doi:10.1002/lno.12175)

117. Tagliabue A, Bowie AR, Boyd PW, Buck KN, Johnson KS, Saito MA. 2017 The integral role of iron in ocean biogeochemistry. *Nature* **543**, 51–59. (doi:10.1038/nature21058)

118. Nicholson S-A, Lévy M, Jouanno J, Capet X, Swart S, Monteiro PMS. 2019 Iron supply pathways between the surface and subsurface waters of the Southern Ocean: from winter entrainment to summer storms. *Geophys. Res. Lett.* **46**, 14 567–14 575. (doi:10.1029/2019GL084657)

119. Laufkötter C *et al.* 2015 Drivers and uncertainties of future global marine primary production in marine ecosystem models. *Biogeosciences* **12**, 6955–6984. (doi:10.5194/bg-12-6955-2015)

120. Halfter S, Cavan EL, Swadling KM, Eriksen RS, Boyd PW. 2020 The role of zooplankton in establishing carbon export regimes in the Southern Ocean – a comparison of two representative case studies in the Subantarctic region. *Front. Mar. Sci.* **7**, 567917. (doi:10.3389/fmars.2020.567917)

121. Chown SL. 2020 Marine food webs destabilized. *Science (1979)* **369**, 770–771. (doi:10.1126/science.abd5739)

122. Nicholson S-A, Lévy M, Llort J, Swart S, Monteiro PMS. 2016 Investigation into the impact of storms on sustaining summer primary productivity in the Sub-Antarctic Ocean. *Geophys. Res. Lett.* **43**, 9192–9199. (doi:10.1002/2016GL069973)

123. Uchida T, Balwada D, P. Abernathey R, A. McKinley G, K. Smith S, Lévy M. 2020 Vertical eddy iron fluxes support primary production in the open Southern Ocean. *Nat. Commun.* **11**, 1125. (doi:10.1038/s41467-020-14955-0)

124. Wei L, Qin T. 2016 Characteristics of cyclone climatology and variability in the Southern Ocean. *Acta Oceanol. Sin.* **35**, 59–67. (doi:10.1007/s13131-016-0913-y)

125. Setzer AW, Kayano MT, Oliveira MR, Ceron WL, Rosa MB. 2022 Increase in the number of explosive low–level cyclones around King George Island in the last three decades. *An Acad. Bras. Cienc.* **94**. (doi:10.1590/0001-3765202220210633)

126. Shaw TA, Miyawaki O, Donohoe A. 2022 Stormier Southern Hemisphere induced by topography and ocean circulation. *Proc. Natl Acad. Sci. USA* **119**, e2123512119. (doi:10.1073/pnas.2123512119)

127. Zhang Y, Chambers D, Liang X. 2021 Regional trends in southern ocean eddy kinetic energy. *J. Geophys. Res. Oceans* **126**, e2020JC016973. (doi:10.1029/2020JC016973)

128. Beech N, Rackow T, Semmler T, Danilov S, Wang Q, Jung T. 2022 Long-term evolution of ocean eddy activity in a warming world. *Nat. Clim. Change* **12**, 910–917. (doi:10.1038/s41558-022-01478-3)

129. Risien CM, Chelton DB. 2008 A global climatology of surface wind and wind stress fields from eight years of QuikSCAT scatterometer data. *J. Phys. Oceanogr.* **38**, 2379–2413. (doi:10.1175/2008JPO3881.1)

130. Lin X, Zhai X, Wang Z, Munday DR. 2018 Mean, variability, and trend of southern ocean wind stress: role of wind fluctuations. *J. Clim.* **31**, 3557–3573. (doi:10.1175/JCLI-D-17-0481.1)

131. Hell MC, Cornuelle BD, Gille ST, Lutsko NJ. 2021 Time-varying empirical probability densities of Southern Ocean Surface winds: linking the leading mode to sam and quantifying wind product differences. *J. Clim.* **34**, 5497–5522. (doi:10.1175/JCLI-D-20-0629.1)

132. Finkel ZV, Beardall J, Flynn KJ, Quigg A, Rees TAV, Raven JA. 2010 Phytoplankton in a changing world: cell size and elemental stoichiometry. *J. Plankton Res.* **32**, 119–137. (doi:10.1093/plankt/fbp098)

133. Henson SA, Cael BB, Allen SR, Dutkiewicz S. 2021 Future phytoplankton diversity in a changing climate. *Nat. Commun.* **12**, 5372. (doi:10.1038/s41467-021-25699-w)

134. Leung SW, Weber T, Cram JA, Deutsch C. 2021 Variable particle size distributions reduce the sensitivity of global export flux to climate change. *Biogeosciences* **18**, 229–250. (doi:10.5194/bg-18-229-2021)

135. Siegel DA, Buesseler KO, Doney SC, Sailley SF, Behrenfeld MJ, Boyd PW. 2014 Global assessment of ocean carbon export by combining satellite observations and food-web models. *Global Biogeochem. Cycles* **28**, 181–196. (doi:10.1002/2013GB004743)

136. Westberry T, Behrenfeld MJ, Siegel DA, Boss E. 2008 Carbon-based primary productivity modeling with vertically resolved photoacclimation. *Global Biogeochem. Cycles* **22**, 1–18. (doi:10.1029/2007GB003078)

137. Kostadinov TS, Siegel DA, Maritorena S. 2009 Retrieval of the particle size distribution from satellite ocean color observations. *J. Geophys. Res. Oceans* **114**, 1–22. (doi:10.1029/2009JC005303)

138. Moutier W, Thomalla JS, Bernard S, Wind G, Ryan-Keogh JT, Smith EM. 2019 Evaluation of chlorophyll-a and POC MODIS Aqua products in the Southern Ocean. *Remote Sens. (Basel).* **11**, 1793. (doi:10.3390/rs11151793)

139. Pope A, Wagner P, Johnson R, Shutler JD, Baeseman J, Newman L. 2017 Community review of Southern Ocean satellite data needs. *Antarct. Sci.* **29**, 97–138. (doi:10.1017/S0954102016000390)

140. Robinson CM, Huot Y, Schuback N, Ryan-Keogh TJ, Thomalla SJ, Antoine D. 2021 High latitude Southern Ocean phytoplankton have distinctive bio-optical properties. *Opt. Express* **29**, 21 084–21 112. (doi:10.1364/OE.426737)

141. Bellacicco M, Volpe G, Briggs N, Brando V, Pitarch J, Landolfi A, Colella S, Marullo S, Santoleri R. 2018 Global distribution of non-algal particles from ocean color data and implications for phytoplankton biomass detection. *Geophys. Res. Lett.* **45**, 7672–7682. (doi:10.1029/2018GL078185)

142. Brewin RJW *et al.* 2011 An intercomparison of bio-optical techniques for detecting dominant phytoplankton size class from satellite remote sensing. *Remote Sens. Environ.* **115**, 325–339. (doi:10.1016/j.rse.2010.09.004)

143. Allison DB, Stramski D, Mitchell BG. 2010 Empirical ocean color algorithms for estimating particulate organic carbon in the Southern Ocean. *J. Geophys. Res. Oceans* **115**, 1–16. (doi:10.1029/2009JC006040)

144. Evers-King H *et al.* 2017 Validation and intercomparison of ocean color algorithms for estimating particulate organic carbon in the oceans. *Front. Mar. Sci.* **4**, 251. (doi:10.3389/fmars.2017.00251)

145. Soppa M, Dinter T, Taylor B, Peeken I, Bracher A. 2012 Comparison of remotely sensed phytoplankton functional types retrievals in the Southern Ocean. In *The 44th Int. Liege Colloquium On Ocean Dynamics, Liege, Belgium, 7–11 May 2012*. Bremerhaven, Germany: AWI.

146. Kostadinov TS *et al.* 2017 Inter-comparison of phytoplankton functional type phenology metrics derived from ocean color algorithms and earth system models. *Remote Sens. Environ.* **190**, 162–177. (doi:10.1016/j.rse.2016.11.014)

147. Rudnick DL, Davis RE, Eriksen CC, Fratantoni DM, Perry MJ. 2004 Underwater gliders for ocean research. *Mar Technol Soc J* **38**, 73–84. (doi:10.4031/002533204787522703)

148. Alkire MB, Lee C, D'Asaro E, Perry MJ, Briggs N, Cetinić I, Gray A. 2014 Net community production and export from Seaglider measurements in the North Atlantic after the spring bloom. *J. Geophys. Res. Oceans* **119**, 6121–6139. (doi:10.1002/2014JC010105)
149. Arteaga LA, Behrenfeld MJ, Boss E, Westberry TK. 2022 Vertical structure in phytoplankton growth and productivity inferred from biogeochemical-argo floats and the carbon-based productivity model. *Global Biogeochem. Cycles* **36**, e2022GB007389. (doi:10.1029/2022GB007389)
150. Thomalla SJ, Ryan-Keogh T. 2023 Code for: understanding the sensitivity of the Southern Ocean Biological Carbon pump to climate change: Insights from a seasonal cycle approach. *Zenodo*. (doi:10.5281/zenodo.7108117)
151. Thomalla SJ *et al.* 2023 Southern Ocean phytoplankton dynamics and carbon export: insights from a seasonal cycle approach. Figshare. (doi:10.6084/m9.figshare.c.6602317)